

Accelerated Process Optimization of Chromatographic Separations Using a Hybrid Modeling Approach

Foteini Michalopoulou*, Maria M. Papathanasiou**

* *The Sargent Centre for Process Systems Engineering, Department of Chemical Engineering, Imperial College London, London, United Kingdom (e-mail: foteini.michalopoulou21@imperial.ac.uk).*

** *The Sargent Centre for Process Systems Engineering, Department of Chemical Engineering, Imperial College London, London, United Kingdom (e-mail: maria.papathanasiou11@imperial.ac.uk)*

Abstract: Chromatographic separation processes are essential for achieving high-purity products in industries such as pharmaceuticals and biotechnology, where complex mixtures such as monoclonal antibodies require precise purification. These processes, such as the twin-column Multicolumn Countercurrent Solvent Gradient Purification (MCSGP), are typically described by nonlinear partial differential and algebraic equations, leading to high computational demands that limit their feasibility for real-time optimization. In this work, we develop a hybrid modeling approach that combines artificial neural networks (ANNs) with process knowledge to capture the nonlinear dynamics of the twin-column MCSGP system efficiently. By retaining the mechanistic separation isotherm while eliminating the need for spatial discretization, the model reduces computational effort substantially, achieving cyclic steady state (CSS) predictions in a fraction of the time required by the respective high-fidelity model. The hybrid model is integrated within a Bayesian optimization (BO) framework to maximize process yield while meeting stringent product purity requirements. A comparative analysis with both data-driven and high-fidelity models demonstrates that the hybrid model provides a computationally efficient, accurate alternative suitable for real-time applications in continuous chromatography.

Keywords: machine learning, artificial intelligence, artificial neural networks, data-driven models, hybrid models, optimization, computing and systems engineering.

1. INTRODUCTION

Chromatographic separation processes play a pivotal role across various industries, particularly within pharmaceuticals and biotechnology, where they are commonly employed for the purification of complex mixtures such as monoclonal antibodies, peptides, and small molecules (Di Stefano et al., 2012; Pinto et al., 2015). These processes are essential for achieving the high levels of product purity required to meet stringent regulatory and quality standards (Müller-Späth et al., 2013). However, the intricate dynamics of chromatographic separations - characterized by nonlinear adsorption behavior, mass transfer limitations, and complex fluid interactions - pose considerable challenges for process optimization and control (Papathanasiou & Kontoravdi, 2020). Limited access to real-time process analytical technologies (PATs) further complicates the task, as it restricts the ability to monitor and adjust critical variables on-line, during process operation (Asnin, 2016). As a result, the drive for efficient, real-time optimization of chromatographic processes has become a central focus, with the potential to substantially impact both process productivity and economic viability.

Mechanistic models have traditionally been the primary approach for capturing the detailed behavior of chromatographic processes (Kumar et al., 2021). These models, grounded in fundamental principles, use Partial Differential and Algebraic Equations (PDAEs) to represent

mass transfer, adsorption, and fluid dynamics accurately (De Luca et al., 2020). However, the high computational cost of solving PDAEs often limits these models' applicability in real-time optimization frameworks, where rapid decision-making is essential (Daoutidis et al., 2024). Consequently, there is growing interest in developing alternative modeling approaches that can reduce computational complexity without compromising predictive accuracy, especially for dynamic process scenarios (Osberghaus et al., 2012).

In this context, data-driven and hybrid modeling approaches have emerged as promising alternatives (Silva et al., 2024; Wang et al., 2017). Purely data-driven models can approximate process behaviors directly from historical and simulated process data, yielding computational efficiency suited for optimization tasks (Michalopoulou & Papathanasiou, 2024; Webb et al., 2009). Nevertheless, data-driven models typically rely on correlations within a defined training range, which can limit their robustness and accuracy when extrapolating beyond this range, particularly in nonlinear, multicomponent systems like chromatographic separations (Mouellef et al., 2023). Hybrid models, on the other hand, integrate mechanistic insights, often through selected equations or process characteristics, with the computational flexibility of data-driven techniques (Narayanan et al., 2021). By combining the fidelity of mechanistic models with the adaptability of data-driven methods, hybrid models can retain critical process dynamics while achieving significant reductions in computational

demands (Joshi et al., 2017). This integration makes hybrid models especially suitable for real-time process optimization, where computational efficiency and adaptability to variable conditions are paramount (Ding et al., 2023).

This paper focuses on the implementation of data-driven and hybrid models in the optimization of the twin-column Multicolumn Countercurrent Solvent Gradient Purification (MCSGP) process. Widely used for monoclonal antibody purification, the MCSGP process exemplifies the complexities involved in chromatographic separation systems. A hybrid model of the process is developed that leverages mechanistic knowledge to preserve key process characteristics while reducing computational demands through data-driven elements. The developed model is implemented in a process optimization framework to maximize process yield and ensure high product purity, addressing core performance metrics in chromatography. Its performance is compared to a previously published data-driven model of the process (Michalopoulou & Papathanasiou, 2024), allowing for an in-depth analysis of computational efficiency, predictive accuracy, and optimization capability. Through this comparative analysis, we evaluate the performance of the hybrid model against the fully data-driven model and assess their respective capabilities in real-time optimization.

2. CASE STUDY: TWIN-COLUMN MCSGP

We focus on the twin-column MCSGP process, a critical purification step in monoclonal antibody (mAb) production. Originally developed by Aumann & Morbidelli (2007), the MCSGP process is a semicontinuous ion-exchange chromatography technique featuring two identical columns that alternate between isolated batch mode (B phases) and interconnected operation (I phases). This configuration facilitates the continuous separation of a complex three-component mixture introduced in the feed (F) - comprising weak impurities (W), the target product (P), and strong impurities (S) - by leveraging a modifier (M) gradient that adjusts the charge on the chromatographic medium to enhance separation specificity.

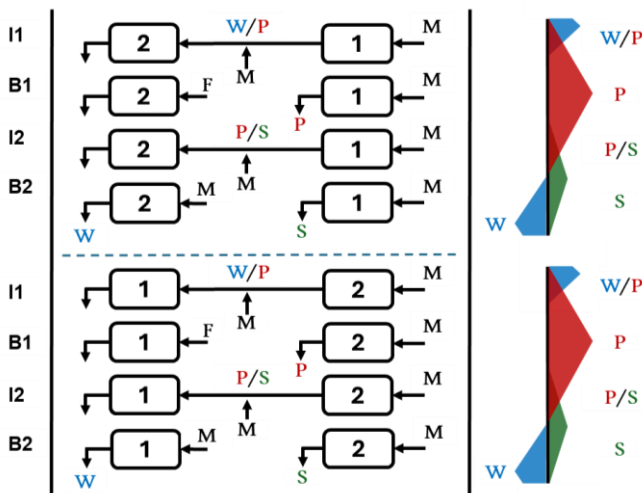


Figure 1: Schematic overview of a cycle of the twin-column MCSGP process.

The MCSGP process is executed through four distinct process steps (Figure 1), which are carried out in a synchronized, alternating manner across the two columns. This alternating sequence allows each column to cycle through these four steps, achieving continuous operation at cyclic steady state (CSS) by recycling partially separated streams and adapting the modifier gradient to enable high-purity separation.

3. METHODOLOGY

3.1 High-Fidelity Process Model and Complexity Analysis

To simulate the MCSGP process, a high-fidelity model developed by (Müller-Spätth et al., 2008) is used. The experimentally validated model (Müller-Spätth et al., 2010), employs a detailed lumped kinetics framework, with a competitive Bi-Langmuir isotherm, to describe species concentrations in both liquid and solid phases along the column length. Represented as a one-dimensional system, the model utilizes spatial discretization with 50 discretization points, leading to a system of over 3,300 variables and more than 4,000 differential and algebraic equations. A total of 11 process cycles are required for the model to reach CSS, which adds significant computational burden. For a detailed description of the model and the equations that comprise it, the reader is referred to Papathanasiou et al. (2016).

The main source of computational complexity and cost in the high-fidelity model arises from the need to discretize the partial differential equations describing the liquid (1) and solid (2) phase concentrations in the spatial and temporal domains.

$$\frac{\partial c(z,t)_{i,h}}{\partial t} = D_{ax} \frac{\partial^2 c(z,t)_{i,h}}{\partial z^2} - \frac{Q_h}{A_{col} \varepsilon_i} \frac{\partial c(z,t)_{i,h}}{\partial z} - \frac{(1 - \varepsilon_i)}{\varepsilon_i} \frac{\partial q(z,t)_{i,h}}{\partial t} \quad (1)$$

$$\frac{\partial q(z,t)_{i,h}}{\partial t} = k_i (q^*(c(z,t)_{i,h}) - q(z,t)_{i,h}) \quad (2)$$

where, t is the time, z the column length, i the components in order of elution - (1) modifier, (2) weak impurities, (3) product, and (4) strong impurities - and h the column index. $c(z,t)_{i,h}$, $q(z,t)_{i,h}$ and $q^*(c(z,t)_{i,h})$ are the liquid, solid and solid equilibrium phase concentrations of component i in column h respectively. A_{col} and Q_h are the column cross-section and the volumetric flowrate of column h , while ε_i and k_i are the column porosity and the lumped mass transfer coefficient of component i respectively.

This spatial discretization requirement adds a high number of variables and equations, which increases simulation time and limits the model's feasibility for real-time applications. Previous work (Michalopoulou & Papathanasiou, 2024) has addressed this challenge by developing data-driven models to eliminate spatial discretization and, consequently, the need for complex partial differential-algebraic equations (PDAEs) in the model formulation. Following this approach, the hybrid model aims to eliminate the spatial discretization of the partial differential equations while retaining essential mechanistic knowledge about the separation process to ensure predictive accuracy.

The primary question in developing the hybrid model, therefore, is determining what critical information can be preserved to maintain an accurate representation of the separation process without relying on spatial discretization. To achieve this, the hybrid model retains the separation isotherm (3), a fundamental element that governs the adsorption dynamics of solutes within the chromatographic columns. By preserving the separation isotherm in the hybrid framework, the model can capture key adsorption and competition behaviors between species, ensuring that the essential dynamics of the MCSGP process are represented without the computational overhead associated with full spatial discretization.

$$q^*(c(z, t)_{i,h}) = \frac{c_{i,h} \cdot H_{i,h}^I}{1 + \sum_{i=2}^{n_{comp}} \frac{c_{i,h} \cdot H_{i,h}^I}{q_{i,h}^I}} + \frac{c_{i,h} \cdot H_{i,h}^{II}}{1 + \sum_{i=2}^{n_{comp}} \frac{c_{i,h} \cdot H_{i,h}^{II}}{q_{i,h}^{II}}} \quad (3)$$

where, $H_{i,h}^I$ and $H_{i,h}^{II}$ the Henry constants, and $q_{i,h}^I$ and $q_{i,h}^{II}$ are the saturation capacities, of component i in column h , for the adsorption sites 1 and 2 respectively.

3.2 Hybrid Model Structure

Based on the complexity analysis and the objective of reducing computational cost, a hybrid model is developed to eliminate spatial discretization while retaining essential process information. The model aims to capture the dynamics of the MCSGP process at CSS, thus requiring only a single-cycle simulation to predict system behavior without the need for multiple cycle repetitions. To maintain accurate separation characteristics without spatial discretization, the hybrid model incorporates the separation isotherm, which governs competitive adsorption dynamics and captures essential system interactions.

To accomplish this, the hybrid model integrates the mechanistic knowledge with an artificial neural network (ANN), trained to predict the outlet liquid phase concentrations of the separation species, based on key operating conditions such as flowrates, feed composition, and initial modifier concentration (Figure 2). In addition to these fixed process conditions, the ANN receives as inputs at each timestep (t) the inlet concentrations of the modifier and separation species, as well as the solid-phase equilibrium concentrations from the previous timestep ($t-dt$). This approach allows the ANN to approximate concentration profiles per timestep while eliminating the need for spatial discretization and performing calculations only at the column outlet. By including these equilibrium concentrations as inputs, the ANN captures essential adsorption dynamics and competitive interactions that are integral to accurately predicting outlet concentrations at CSS. With this setup, the hybrid model relies only on experimentally determined constants and coefficients, and the embedded isotherm, allowing it to achieve predictive accuracy with significantly reduced complexity.

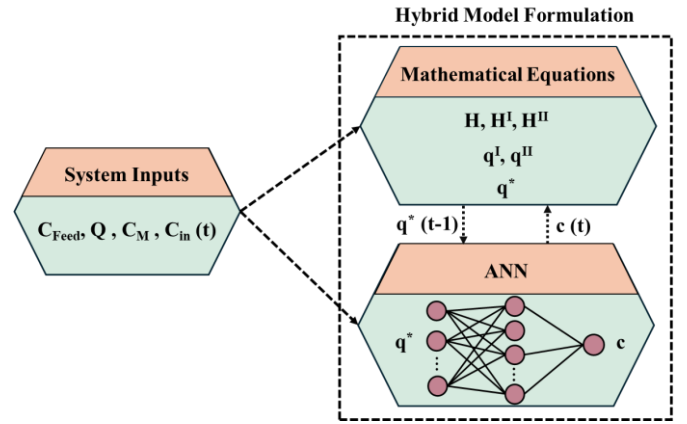


Figure 2: Schematic overview of the structure of the hybrid model.

3.3 Synthetic Data Generation

To train the ANN component of the hybrid model, synthetic data are generated using the high-fidelity model, simulating the MCSGP system across a range of operating conditions. Nine key input variables that include the flowrates, feed composition, and modifier concentrations, are varied using a quasi-random Sobol sequence to sample the input space within the validation range of the high-fidelity model (Michalopoulou & Papathanasiou, 2024). Each simulation is conducted until CSS, at which point an entire cycle monitored, yielding 27,200 data points across 400 process cycles. This dataset includes both inlet and outlet liquid phase concentrations, along with solid phase equilibrium concentrations, providing a comprehensive basis for ANN training.

3.4 Process Optimization Framework

To evaluate the hybrid model's utility in optimizing the MCSGP process, it is embedded within a process optimization framework designed to maximize process yield (4) while meeting a product purity (5) threshold of 98% (Müller-Späh et al., 2013). Bayesian Optimization (BO) is employed to adjust the flowrates across the different phases of the MCSGP system, which directly impact the process yield and purity.

$$Y_j = \frac{C_{avP,s,j}}{C_p^{feed}} \quad (4)$$

$$Pur_{av,j} = \frac{C_{avP,s,j}}{C_{avW,s,j} + C_{avP,s,j} + C_{avS,s,j}} \quad (5)$$

where, j is the cycle index, s is the outlet stream, C_p^{feed} is the product concentration in the feed stream introduced to the system, and $C_{avi,s,j}$ is the average concentration of component i in stream s during cycle j . The optimization problem is formulated as follows:

$$\begin{aligned} \min_q (F = -Y_j) \\ \text{s.t. } 0.1 \leq Q_B \leq 1 \\ 0.1 \leq Q_{II} \leq 1 \\ 0.1 \leq Q_{I2} \leq 1 \\ Pur_{av,j} \geq 98\% \end{aligned}$$

where, Q_B the flowrates implemented during the batch phases B1 and B2 of the MCSGP operation, and Q_{I1} and Q_{I2} the flowrates implemented during the interconnected phases I1 and I2 of the process operation respectively (Müller-Spáth et al., 2008).

4. RESULTS AND DISCUSSION

4.1 Hybrid Model Validation

A hybrid model of the MCSGP process is developed based on the presented methodology. The ANN integrated in the model is trained using the ReLU (Rectified Linear Unit) activation function and BO with early stopping is employed to tune its hyperparameters, resulting in a network of 3 hidden layers, 98 neurons per layer and a learning rate of $8.04 \cdot 10^{-3}$. The resulting hybrid model is validated by comparing its CSS predictions to those of the high-fidelity model across a range of operating conditions. Both interpolation and extrapolation accuracy are evaluated to assess the hybrid model’s reliability within the trained input space of the operating conditions and its performance when applied beyond the direct training range. Ten new sets of input data are generated using the high-fidelity process model, half within the training bounds of the hybrid model to test interpolation and the other half outside the bounds to test extrapolation. Two performance metrics are used to evaluate the accuracy of the model; the root mean squared error (RMSE) and the mean absolute percentage error (MAPE). Further to that, the metrics are used to assess the model accuracy for one entire process cycle at CSS, as well as specifically during the product collection window, wherein the key performance indicators (KPIs) of the process - the product purity and process yield - are calculated. Results, presented in Table 1, show that the hybrid model closely matches the high-fidelity predictions for key concentration profiles in both interpolation and extrapolation scenarios, with average error percentages remaining within acceptable bounds for practical applications.

Table 1: Interpolation and extrapolation performance of the hybrid model during one process cycle at CSS and during the product collection window.

	Metric	Interpolation	Extrapolation
Process Cycle at CSS	RMSE (mg/ml)	0.019	0.044
	MAPE (%)	4.0	9.0
Product Collection	RMSE (mg/ml)	0.007	0.038
	MAPE (%)	2.0	7.0

In addition to prediction accuracy, the computational efficiency of the hybrid model was evaluated by comparing the time required for a single-cycle CSS prediction with that of the high-fidelity model. As a result, the hybrid model achieved a 97% reduction in computational time, requiring only a fraction of the processing time needed by the high-fidelity model to reach and maintain CSS. This efficiency stems from the hybrid model’s elimination of spatial discretization and complex partial differential equation solutions, enabling a direct CSS prediction with minimal computational overhead.

4.2 Process Optimization

Following validation, the hybrid model is implemented within a process optimization framework to determine optimal flowrate settings while maintaining the feed composition and the initial modifier concentration at nominal values. For a comprehensive comparison, optimization is also conducted using a fully data-driven model developed using the same amount of data (Michalopoulou & Papathanasiou, 2024) and the high-fidelity model of the process. The optimized flowrate settings identified by each model are then implemented in the high-fidelity model to assess the resulting process yield and product purity, enabling a direct comparison of optimization effectiveness across the three models.

Each optimization is performed within a fixed timeframe of one hour to evaluate how effectively each model can identify optimal operating conditions under a realistic constraint for online implementation. Given that a process cycle has a duration that exceeds one hour, this approach ensures that the optimization can be conducted within a single cycle to determine the optimal flowrates for the subsequent process cycle. Under this framework, the number of iterations each model completes within the allocated time varies significantly due to differences in computational complexity. The high-fidelity model completes 30 iterations, while the hybrid model performs approximately 600 iterations, and the data-driven model achieves almost 3600 iterations. To assess how well the models approximate the actual optimal operating conditions, a separate optimization was performed using the high-fidelity process model, where computational time was not restricted. This true optimum serves as a benchmark for evaluating the effectiveness of the surrogate models. The resulting optimal flowrate settings and corresponding KPIs are summarized in Table 2.

Table 2: Optimal flowrates identified during the time-constrained process optimization performed by the three models of the process - high-fidelity, hybrid and data driven - and resulting KPIs calculated by the high-fidelity model, along with the true optimum calculated by the high-fidelity model.

	Data-Driven	Hybrid	High-Fidelity	True Optimum
Q_B (mL/min)	0.84	0.96	1	0.87
Q_{I1} (mL/min)	0.69	0.65	0.61	0.71
Q_{I2} (mL/min)	0.24	0.24	0.24	0.24
Purity (%)	98	98	98	98
Yield (%)	79	82	78	86

During the optimization, the algorithm adjusts the three key flowrates within a range of 0.1–1 mL/min, allowing for a broad exploration of the parameter space. Despite completing significantly fewer iterations than the data-driven model, the hybrid model achieved the highest process yield (82%), outperforming both the data-driven model (79%) and the high-fidelity model (78%), while still maintaining the required product purity of 98%. Importantly, both the hybrid and data-driven models identified conditions that are closer to the true optimum compared to the one-hour high-fidelity optimization.

5. CONCLUSIONS AND OUTLOOK

The high-fidelity model, despite being the most accurate representation of the process, was unable to explore enough of the parameter space in just 30 iterations, leading to a suboptimal yield. The data-driven model, despite completing the highest number of iterations, did not benefit from mechanistic insights, resulting in a slightly lower yield than the hybrid model. These results highlight the ability of the hybrid model to efficiently navigate the optimization space and identify operating conditions that maximize yield within the given time constraint while remaining closely aligned with the true optimum. The resulting elution profiles for the three components of the separation based on the optimal flowrates identified by each model are presented in Figure 3.

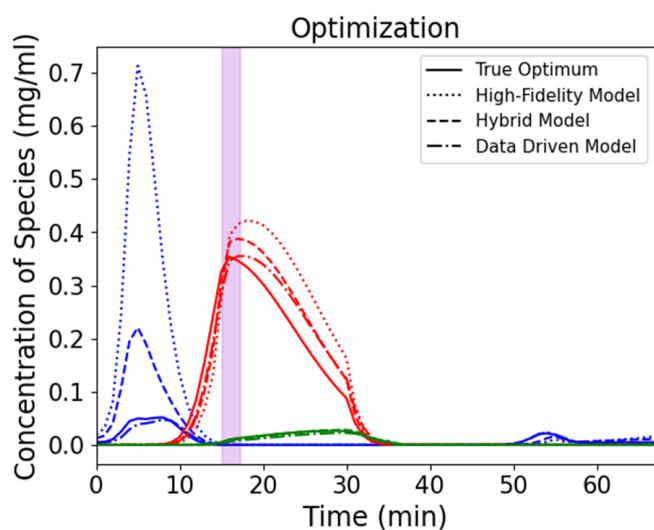


Figure 3: Comparison of the optimal elution profiles of the three separation species - weak impurities (blue), product (red), and strong impurities (green) - as optimized by the high-fidelity, hybrid and data driven models, and calculated at CSS using the high-fidelity process model. The product collection window is highlighted in purple.

The elution profiles in Figure 3 illustrate the concentration trajectories of the weak impurities, product, and strong impurities at CSS, as calculated using the optimal flowrates identified by each model. A notable difference is observed in the weak impurities, where the high-fidelity model exhibits an accumulation of these species in the system, a behavior that is significantly reduced in both the hybrid and data-driven models. This accumulation suggests that the high-fidelity model's optimization, due to its limited iterations, was unable to fully refine flowrate adjustments to improve impurity clearance. Conversely, the hybrid and data-driven models effectively reduced impurity retention.

Most importantly, the elution profiles obtained using the hybrid and data-driven models are more closely aligned with the true optimum than those produced by the high-fidelity model under time constraint (Figure 3). This confirms that both surrogate models are not only computationally efficient but also highly effective in identifying near-optimal conditions in a fraction of the time required for the timewise unconstrained high-fidelity optimization. As such, they can be used in applications requiring quick and reliable predictions.

In this work, a hybrid model was developed and validated for the twin-column Multicolumn Countercurrent Solvent Gradient Purification (MCSGP) process, with the goal of achieving efficient and accurate process optimization. The hybrid model combined mechanistic knowledge, through the separation isotherm, with data-driven elements, via artificial neural networks (ANNs), allowing it to predict cyclic steady state (CSS) behavior directly without spatial discretization. The model was embedded in a Bayesian optimization (BO) setup to determine optimal flowrate settings, and its performance was compared with that of a fully data-driven model and of a high-fidelity model of the process. The model demonstrated increased computational efficiency and robustness, establishing it as a viable alternative to high-fidelity modeling for real-time applications.

The comparative analysis between the hybrid, data-driven, and high-fidelity models illustrated the strengths of the hybrid approach in reducing computational complexity while retaining high accuracy. The hybrid model achieved high accuracy when compared to the high-fidelity model, capturing essential dynamics with an accuracy of over 96% in interpolation and 91% in extrapolation throughout the process cycle and a substantial reduction of 97% in computational cost and simulation time requirements. Thus, the hybrid model's performance highlighted its suitability for online applications, where the balance between predictive accuracy and computational efficiency is critical.

In terms of process optimization, the results demonstrated that the hybrid model can offer a practical solution for applications requiring real-time adjustments, as it delivered accurate predictions while maintaining computational efficiency. The hybrid model outperformed the time-constrained high-fidelity optimization, as well as the data-driven optimization, achieving a higher yield (82%) while closely approximating the true optimum (86%). By integrating mechanistic insights with data-driven adaptability, the hybrid model efficiently explored the parameter space, identifying optimal conditions faster and more accurately than the high-fidelity and fully data-driven models respectively. Its ability to achieve near-optimal performance within the duration of a single process cycle makes it particularly valuable for continuous operation, where real-time optimization is required to dynamically adjust flowrates and maximize product recovery while maintaining strict purity standards.

Future work could explore the application of transfer learning to extend the hybrid model's applicability to similar chromatographic processes, reducing the need for extensive retraining when adapting to new systems. This approach would leverage the knowledge embedded in the current model to accelerate the development of predictive models for other separation processes with analogous dynamics. Additionally, integrating reinforcement learning (RL) could enhance the framework's ability to achieve closed-loop process control. By employing RL agents trained to optimize operational parameters in response to real-time feedback, the system could dynamically adjust flowrates and other critical variables to maintain product purity and yield under fluctuating feed

compositions or operational disturbances. These extensions could solidify the hybrid model's role as a powerful, computationally efficient solution for advanced process control in chromatography and similar applications.

ACKNOWLEDGEMENTS

Funding from the UK Engineering & Physical Sciences Research Council (EPSRC) for the i-PREDICT: Integrated Adaptive Process Design and Control (Grant reference: EP/W035006/1) is gratefully acknowledged. FM is grateful for the Burkett Scholarship awarded by the Department of Chemical Engineering, Imperial College London.

REFERENCES

- Asnin, L. D. (2016). Peak measurement and calibration in chromatographic analysis. *TrAC Trends in Analytical Chemistry*, 81, 51–62.
- Aumann, L., & Morbidelli, M. (2007). A continuous multicolumn countercurrent solvent gradient purification (MCSGP) process. *Biotechnology and Bioengineering*, 98(5), 1043–1055.
- Daoutidis, P., Lee, J. H., Rangarajan, S., Chiang, L., Gopaluni, B., Schweidtmann, A. M., Harjunkoski, I., Mercangöz, M., Mesbah, A., Boukouvala, F., Lima, F. V., del Rio Chanona, A., & Georgakis, C. (2024). Machine learning in process systems engineering: Challenges and opportunities. *Computers & Chemical Engineering*, 181, 108523.
- De Luca, C., Felletti, S., Macis, M., Cabri, W., Lievore, G., Chenet, T., Pasti, L., Morbidelli, M., Cavazzini, A., Catani, M., & Ricci, A. (2020). Modeling the nonlinear behavior of a bioactive peptide in reversed-phase gradient elution chromatography. *Journal of Chromatography A*, 1616, 460789.
- Di Stefano, V., Avellone, G., Bongiorno, D., Cunsolo, V., Muccilli, V., Sforza, S., Dossena, A., Drahos, L., & Vékey, K. (2012). Applications of liquid chromatography–mass spectrometry for food analysis. *Journal of Chromatography A*, 1259, 74–85.
- Ding, C., Gerberich, C., & Ierapetritou, M. (2023). Hybrid model development for parameter estimation and process optimization of hydrophobic interaction chromatography. *Journal of Chromatography A*, 1703, 464113.
- Joshi, V. S., Kumar, V., & Rathore, A. S. (2017). Optimization of ion exchange sigmoidal gradients using hybrid models: Implementation of quality by design in analytical method development. *Journal of Chromatography A*, 1491, 145–152.
- Kumar, V., Leweke, S., Heymann, W., von Lieres, E., Schlegel, F., Westerberg, K., & Lenhoff, A. M. (2021). Robust mechanistic modeling of protein ion-exchange chromatography. *Journal of Chromatography A*, 1660, 462669.
- Michalopoulou, F., & Papathanasiou, M. M. (2024). Assessment of data-driven modeling approaches for chromatographic separation processes. *AIChE Journal*, e18600.
- Mouellef, M., Vetter, F. L., & Strube, J. (2023). Benefits and Limitations of Artificial Neural Networks in Process Chromatography Design and Operation. *Processes* 2023, Vol. 11, Page 1115, 11(4), 1115.
- Müller-Späth, T., Aumann, L., Melter, L., Ströhlein, G., & Morbidelli, M. (2008). Chromatographic separation of three monoclonal antibody variants using multicolumn countercurrent solvent gradient purification (MCSGP). *Biotechnology and Bioengineering*, 100(6), 1166–1177.
- Müller-Späth, T., Krättli, M., Aumann, L., Ströhlein, G., & Morbidelli, M. (2010). Increasing the activity of monoclonal antibody therapeutics by continuous chromatography (MCSGP). *Biotechnology and Bioengineering*, 107(4), 652–662.
- Müller-Späth, T., Ströhlein, G., Lyngberg, O., & Maclean, D. (2013). Enabling high purities and yields in therapeutic peptide purification using multicolumn countercurrent solvent gradient purification. *Chimica Oggi/Chemistry Today*, 31(5), 56–60.
- Narayanan, H., Luna, M., Sokolov, M., Arosio, P., Butté, A., & Morbidelli, M. (2021). Hybrid Models Based on Machine Learning and an Increasing Degree of Process Knowledge: Application to Capture Chromatographic Step. *Industrial and Engineering Chemistry Research*, 60(29), 10466–10478.
- Osberghaus, A., Hepbildikler, S., Nath, S., Haindl, M., von Lieres, E., & Hubbuch, J. (2012). Optimizing a chromatographic three component separation: A comparison of mechanistic and empiric modeling approaches. *Journal of Chromatography A*, 1237, 86–95.
- Papathanasiou, M. M., Avraamidou, S., Oberdieck, R., Mantalaris, A., Steinebach, F., Morbidelli, M., Mueller-Spaeth, T., & Pistikopoulos, E. N. (2016). Advanced control strategies for the multicolumn countercurrent solvent gradient purification process. *AIChE Journal*, 62(7), 2341–2357.
- Papathanasiou, M. M., & Kontoravdi, C. (2020). Engineering challenges in therapeutic protein product and process design. *Current Opinion in Chemical Engineering*, 27, 81–88.
- Pinto, I. F., Aires-Barros, M. R., & Azevedo, A. M. (2015). Multimodal chromatography: debottlenecking the downstream processing of monoclonal antibodies. *Pharmaceutical Bioprocessing*, 3(3), 263–279.
- Silva, T. C., Eppink, M., & Ottens, M. (2024). Digital twin in high throughput chromatographic process development for monoclonal antibodies. *Journal of Chromatography A*, 1717, 464672.
- Wang, G., Briskot, T., Hahn, T., Baumann, P., & Hubbuch, J. (2017). Estimation of adsorption isotherm and mass transfer parameters in protein chromatography using artificial neural networks. *Journal of Chromatography A*, 1487, 211–217.
- Webb, R., Doble, P., & Dawson, M. (2009). Optimisation of HPLC gradient separations using artificial neural networks (ANNs): Application to benzodiazepines in post-mortem samples. *Journal of Chromatography B*, 877(7), 615–620.